JOURNAL OF MATERIALS SCIENCE **38** (2003) 3851 – 3860

# Microanalysis of calcium silicate hydrate gel formed within a geopolymeric binder

C. K. YIP, J. S. J. VAN DEVENTER*
*Department of Chemical and Biomolecular Engineering, The University of Melbourne, Victoria 3010, Australia*
*E-mail: jannie@unimelb.edu.au*

It is possible to have geopolymeric gel and calcium silicate hydrate (CSH) gel forming simultaneously within a single system. Scanning electron microscopy was employed in studying the morphology and elemental composition of the two phases. The elemental composition within the different phases was consistent. However, CSH gel formed in such system had a significantly lower Ca/Si ratio than the CSH commonly formed from the hydration of ordinary Portland cement. In addition, there were some calcium precipitate along the interface between the CSH and geopolymeric gels. It is suggested that the properties (e.g., size, elemental composition) of the geopolymeric and CSH gels forming simultaneously, and the reactivity of the calcium precipitates along the interfacial region, will hold the key in reformulating a new generation of concrete that matches the durability of ancient concrete. A chemical mechanism on how the presence of slag in the alkali activation of metakaolin would lead to the formation of both geopolymeric and CSH gels has been proposed. © *2003 Kluwer Academic Publishers*

## 1. Introduction

In studying the durability of ancient construction material in comparison to their modern counterparts, it has been demonstrated by Glukhovsky [1] that the hydration products of ancient concrete are not limited to the hydration of $C_3S$, $C_2S$, $C_3A$ and $C_4AF$, but also include the hydration of low-basic alkaline or alkali-earth aluminosilicate systems. This low-basic alkaline aluminosilicate system could be viewed as the basic geopolymeric system—amorphous $Na^+$ or $K^+$ aluminosilicate network, commonly synthesised today [2].

Calcium silicate hydrate (CSH) gel and calcium hydroxide are commonly acknowledged to be the major hydration products of modern ordinary Portland cement [3]. Hitherto, no documented research has yet identified a system, in which both CSH gel and geopolymeric gel could be formed simultaneously within a single system based on the hydration process of ordinary Portland cement alone. The lack of durability in modern concrete in comparison to the ancient concrete could be attributed to the inability of the modern cementitious system to form a product that consists of both CSH and geopolymeric gels. In order to understand the chemical mechanism behind the durability of ancient concrete, it is essential to reformulate a system that will favour the formation of both CSH and geopolymeric gels within a single system, so that a direct comparison can be made between ancient concrete and this new modern concrete.

Calcium silicate hydrate is a gel of hydrated $CaO$-$SiO_2$, which is normally non-stoichiometric. It is generally agreed that CSH gel is the major component that contributes to the mechanical strength of cement [3]. In contrast, the formation of the three-dimensional amorphous alkali aluminosilicate network with a general formula of $(Na/K)_n$-$[[$-$Si$-$O_2]_z$-$Al$-$O]_n \cdot wH_2O$ is often argued to be the phase that gives the binding property to the geopolymeric gel [4–7]. The major difference between CSH gel and geopolymeric gel in terms of their elemental composition is calcium. It is anticipated that if enough calcium is added to a geopolymeric system, some forms of CSH gel will be obtained instead, however it is still unclear whether calcium will participate in geopolymerisation in a similar way to sodium or potassium [4, 5, 7, 8]. As a result, an investigation into the role of calcium in dictating the chemical mechanism involved in geopolymerisation and formation of CSH gel will be essential in understanding how the coexistence of the two phases will benefit the properties of the resultant binder.

Numerous studies have been conducted on various metakaolin (MK)/lime (calcium hydroxide) and MK-blended cement systems in recent years [9–14]. It was found that various products, such as CSH gel, geopolymeric gel, $C_2ASH_8$ (stratlinite) and $C_4AH_{13}$ (tetracalcium aluminate hydrate) could be synthesised depending on the alkalinity and the different ratios between the aluminosilicate and calcium sources used. Alonso and

---

*Author to whom all correspondence should be addressed.

Palomo [9, 10], in particular, found that it is possible to have geopolymeric and CSH gels forming simultaneously in a MK/lime system.

The current study describes a microscopic study conducted on a MK/ground granulated blast furnace slag (GGBFS) system. A previous study [15] showed that geopolymeric and CSH gels could be formed simultaneously. Moreover, it was found that the presence of both geopolymeric and CSH gels within a single binder would increase the resultant compressive strength. However, X-ray diffraction (XRD) alone was inconclusive to clearly define the structures of the two phases due to the highly amorphous nature of both raw MK and GGBFS, and the resultant product. The findings from the current microscopic study of such a system are fundamental to any further work on the mechanistic relationships between the geopolymers and CSH.

## 2. Experimental work

### 2.1. Materials

Metakaolin (MK) is a highly reactive metastable clay that is essentially an anhydrous aluminosilicate obtained from calcining kaolin to around 650–700°C [16]. Metakaolin was used in this study as the primary aluminosilicate source because it is widely used as aluminosilicate source in geopolymeric systems as well as a pozzolanic admixture in Portland cement.

Metakaolin used in the synthesis was obtained from ECC International under the brand name of MetaStar 402 with a particle size distribution of 100% <10 microns. This commercial metakaolin was purified before calcination, and it had less than 0.1 wt% of CaO as shown in Table I. It was assumed in this study that all calcium would come from ground granulated blast furnace slag (GGBFS). GGBFS was obtained from Independent Cement with a size distribution of 100% <50 microns. The oxide compositions of the metakaolin and granulated blast furnace slag used are shown in Table I, which were obtained by X-Ray Fluorescence (XRF) analysis, using a Siemens SRS 3000 instrument. Table II shows the different molar ratios between the main oxides of interest in both MK and GGBFS.

The sodium silicate (NaSi) solution used in the experiment was supplied by PQ Australia Sydney under the brand name of Vitrosol N48 (with 28.7 wt% $SiO_2$, 8.9 wt% $Na_2O$ and 62.4 wt% $H_2O$; density 1370 kg/m$^3$). Sodium hydroxide pearl (99% purity) was purchased from Orica Australia. Distilled water was used throughout the experiments.

TABLE I Chemical composition of metakaolin (MK) and ground granulated blast furnace slag (GGBFS) in mass%

| | CaO | $SiO_2$ | $Al_2O_3$ | $Fe_2O_3$ | MgO | $K_2O$ | $Na_2O$ | $SO_3$ |
|---|---|---|---|---|---|---|---|---|
| MK | 0.10 | 54.78 | 40.42 | 0.76 | 0.41 | 2.72 | 0.07 | 0 |
| GGBFS | 43.0 | 34.4 | 14.1 | 0.11 | 6.3 | 0.33 | 0.3 | 0.58 |

TABLE II Elemental analysis of the metakaolin (MK) and ground granulated blast furnace slag (GGBFS)

| Molar ratio | $CaO/SiO_2$ | $Al_2O_3/SiO_2$ | $CaO/Al_2O_3$ |
|---|---|---|---|
| MK | 0.002 | 0.43 | 0.0045 |
| GGBFS | 1.34 | 0.24 | 5.56 |

### 2.2. Synthesis

Sodium hydroxide pearl was mixed with the sodium silicate solution to form alkaline solution with two different molar ratios ($Ms = SiO_2/Na_2O = 2.0$ and 1.2). The hot liquid would then be left overnight to be cooled to ambient temperature.

Samples with six different ratios between MK and GGBFS were synthesised in this study: MK/(MK + GGBFS) being 0, 0.2, 0.4, 0.6, 0.8 and 1. The mass ratios between the alkaline mix (sodium hydroxide and sodium silicate solution) and dry mix (MK and GGBFS) were 1.45 and 1.63 for Ms = 2.0 (M1 to M6) and 1.2 (N1 to N6) respectively. These particular ratios were chosen so as to provide for equal moles of water and soluble silicate present in the structures of all the matrices synthesised. Table III presents a summary of all the matrices synthesised in this study.

MK and GGBFS were mixed thoroughly until a uniform mix was produced. The alkaline mix would then be poured and stirred with the dry mix to form a paste. The paste was typically mixed for 3 min to ensure the mixture was homogeneous. The paste was then poured into cylindrical moulds (50 mm diameter and 100 mm length) and allowed to cure in a laboratory convection oven at 40°C for 24 h before being extracted from the moulds and hardened at room temperature (25°C) for another 13, 27, and 239 days for 14, 28 and 240 days analysis respectively. All samples were cured at atmospheric pressure.

### 2.3. Scanning electron microscopy (SEM)

A Philips XL30 scanning electron microscope, operated at 20 keV was used in analysing the surface morphology of the specimen. EDS (Energy Dispersive Spectroscopy) was used to analyse the elemental composition of the surface of a specimen. A DYNAVAC

TABLE III Composition of different matrices synthesised in this study

| Matrix | MK/(MK + GGBFS) (mass) | $Ms = SiO_2/Na_2O$ (mole) | (NaOH + NaSi)/(MK + GGBFS) (mass) |
|---|---|---|---|
| M1 | 1 | 2.0 | 1.45 |
| M2 | 0.8 | 2.0 | 1.45 |
| M3 | 0.6 | 2.0 | 1.45 |
| M4 | 0.4 | 2.0 | 1.45 |
| M5 | 0.2 | 2.0 | 1.45 |
| M6 | 0 | 2.0 | 1.45 |
| N1 | 1 | 1.2 | 1.63 |
| N2 | 0.8 | 1.2 | 1.63 |
| N3 | 0.6 | 1.2 | 1.63 |
| N4 | 0.4 | 1.2 | 1.63 |
| N5 | 0.2 | 1.2 | 1.63 |
| N6 | 0 | 1.2 | 1.63 |

sputter coater was used in coating the specimen with carbon. Elemental analysis was conducted randomly across the area of interest.

## 3. Results and discussion

### 3.1. Microstructure and hydration products synthesised at Ms = 2.0

Fig. 1 illustrates a common microstructural feature found in a MK/GGBFS system synthesised under low alkalinity (Ms = 2.0). Two separate phases were formed as a result of the alkali activation of metakaolin in the presence of a moderate amount of GGBFS (Matrices M2 to M4).

EDS analysis was conducted on the binder in the two separate phases. The results have shown that the two phases had vastly different elemental composition, where one phase (Area A) consisted mainly of silicon, aluminium and sodium with about 1 mol% of calcium, while the other phase (Area B) was found to be dominated by the presence of silicon and calcium with some sodium and less than 3 mol% of aluminium. Based on the elemental composition of areas A and B, it is suggested that area A consisted mainly of geopolymers, while some forms of calcium silicate hydrate (CSH) gel were the main component in area B.

Fig. 2 shows the same binder (Matrix M2 as shown in Fig. 1) at 240 days, where the coexistence of two separate phases remained a prominent feature. The larger particles present in the calcium phases had various compositions and are enlarged in Fig. 3. These particles were of different size, morphology and with different elemental composition. These particles contained various precipitates, such as calcium hydroxide as well as unreacted MK or GGBFS particles.

The crystalline precipitated phases are expected to be of a very low quantity, therefore their presence cannot be detected by using XRD as their crystalline peaks are of very low intensity [15]. From the elemental analysis of the various particles formed within the calcium rich phase, the larger particles (e.g., particles “C” and “D” in Fig. 3) had a substantially higher $CaO/SiO_2$ ratio than the smaller ones (e.g., particle “E”). The larger calcium particles tended to be situated along the interfacial region between the calcium rich region and the aluminosilicate rich region (Figs 1 and 2). In addition, it is anticipated that the presence of the large quantity of calcium along the interfacial region, could be the result of the precipitation of calcium hydroxide.

As more GGBFS was added to the system, the coexistence of geopolymeric gel and calcium silicate hydrate was still the prominent microscopic feature of the binders synthesised under such condition. However a clear distinction between the two phases could not be observed when more than 80 wt% of GGBFS was used. The major products formed in a high percent GGBFS system were various types of calcium silicate hydrate, calcium aluminate hydrate and calcium aluminosilicate hydrate. However, due to the highly amorphous nature of these products, it was not possible to determine whether phases such as $C_2ASH_8$ and $C_4AH_{13}$ were formed.

### 3.2. Microstructure and hydration products synthesised at Ms = 1.2

The microscopic effect of increasing the concentration of sodium hydroxide on the resultant MK/GGBFS

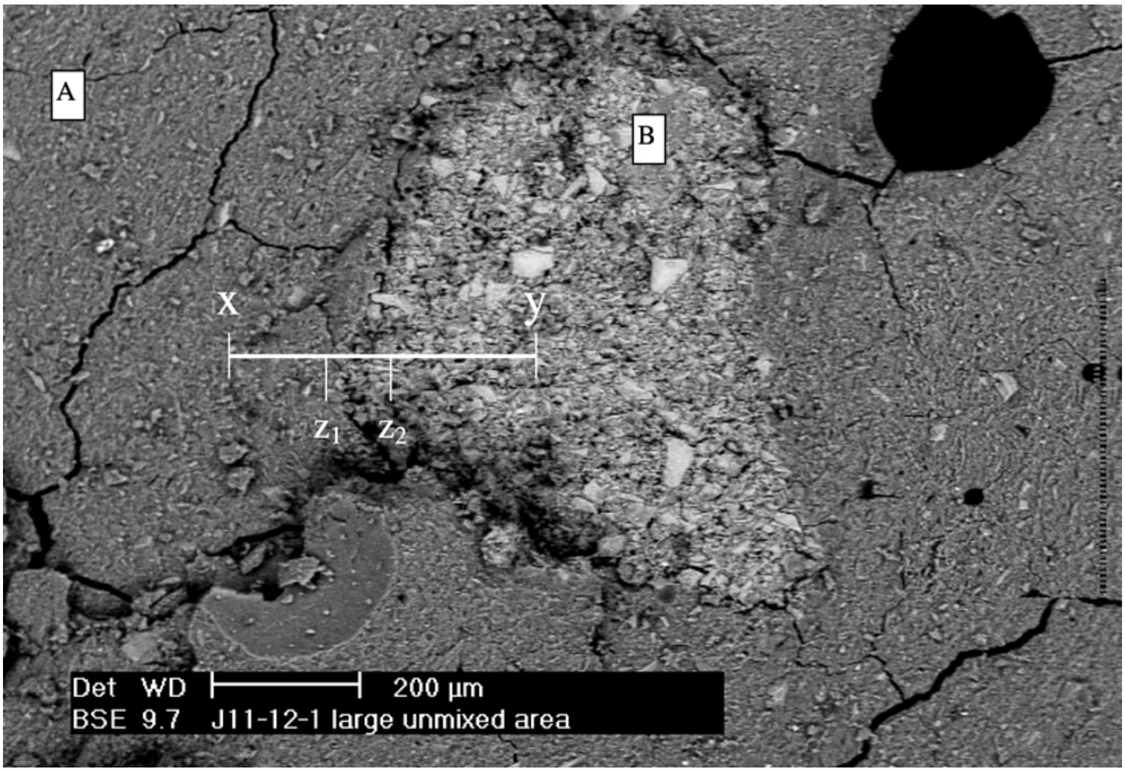

*Figure 1* Scanning electron micrograph of Matrix M2 (20% slag, Ms = 2.0) after 14 days. Identification of the different phases: A-geopolymeric binder with low content of calcium; B-calcium silicate hydrate with a small proportion of aluminium. An elemental line scan was conducted on x–y (see Fig. 5). The interfacial region is marked $z_1$–$z_2$.

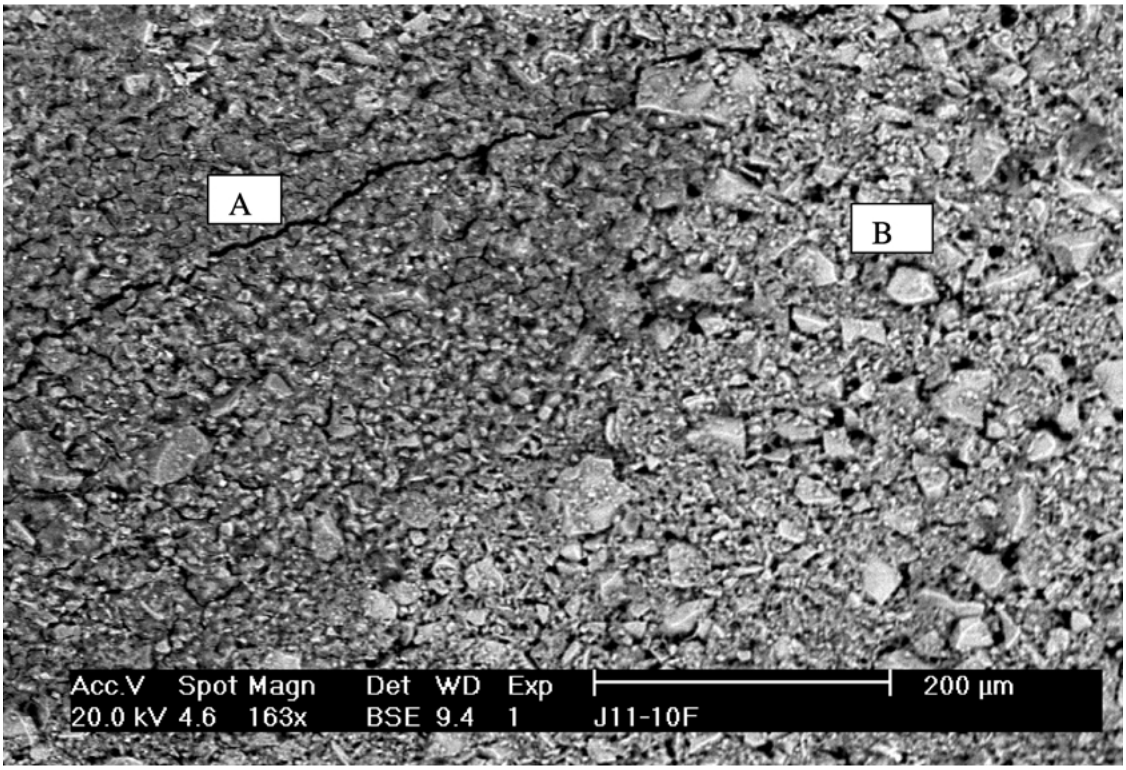

*Figure 2* Scanning electron micrograph of Matrix M2 (20% slag, Ms = 2.0) after 240 days. Identification of the different phases: A-geopolymeric binder with low content of calcium; B-calcium silicate hydrate with a small proportion of aluminium.

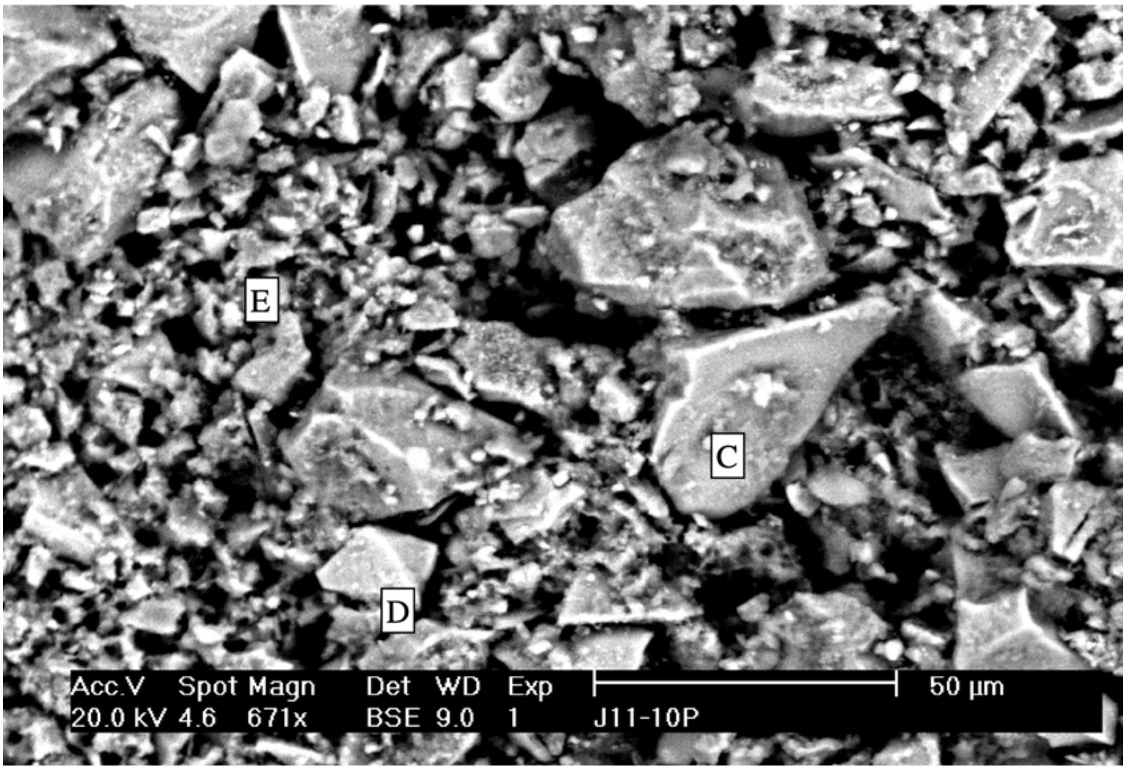

*Figure 3* Scanning electron micrograph of Sample M2 (20% slag, Ms = 2.0) after 240 days, showing magnification of area B in Fig. 2. The particle marked C is identified as a type of calcium silicate with some aluminium in its composition ($CaO/SiO_2 = 1.32$, $Al_2O_3/Na_2O = 2.5$ and $Al_2O_3/SiO_2 = 0.2$) with particle size in the range of 30–50 $\mu$m. The particle marked D is identified as some form of calcium silicate with some aluminium in its composition ($CaO/SiO_2 = 1.8$, $Al_2O_3/Na_2O = 2.0$ and $Al_2O_3/SiO_2 = 0.2$) with size in the range of 20–30 $\mu$m. The calcium content in particles similar to "D" is more than in "C". The particle marked E is identified as some form of aluminosilicate with traces of calcium in its composition ($CaO/SiO_2 = 0.43$, $Al_2O_3/Na_2O = 2.3$ and $Al_2O_3/SiO_2 = 0.26$) with size of about 5 $\mu$m.

binder was studied. Matrices (N1 to N6) were synthesised with the same MK and GGBFS composition as Matrices M1 to M6 but a lower $SiO_2/Na_2O$ ratio (Ms = 1.2). It was found that the coexistence of two separate phases was no longer the dominant microscopic feature of the resultant binder, as shown in the binder synthesised using Ms = 2.0, unless a substantial amount of GGBFS (Matrices N4) was used initially.

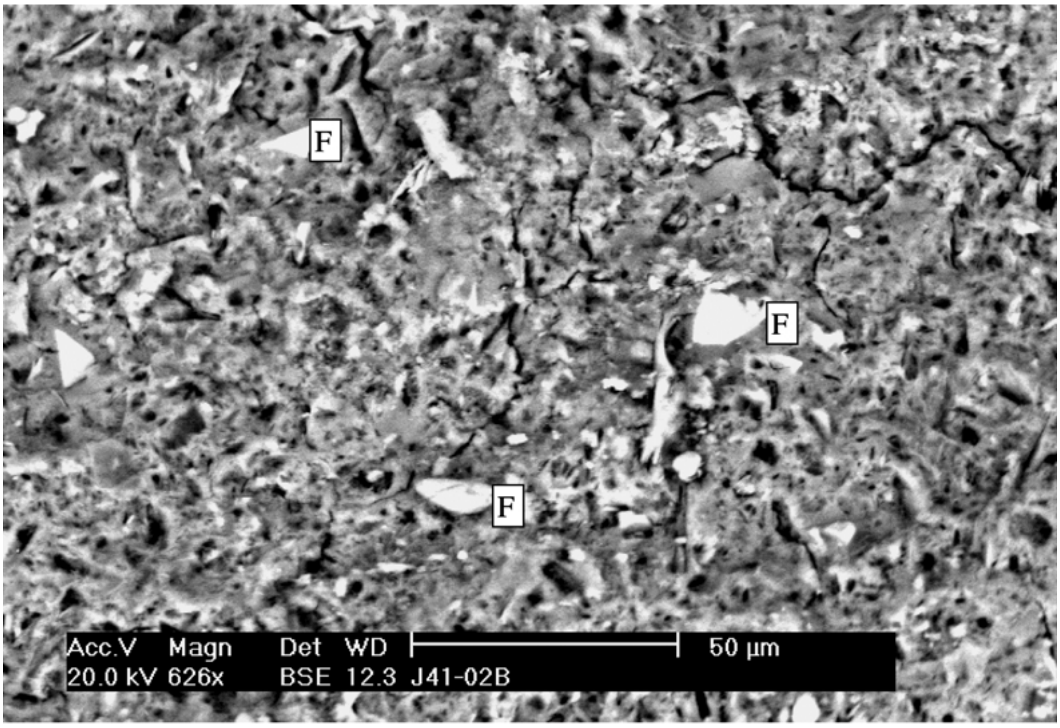

*Figure 4* Scanning electron micrograph of Matrix N2 (20% slag, Ms = 1.2) after 14 days. A clear CSH phase could not be observed in such binder, instead scattering of calcium precipitates (bright white areas, marked "F", <10 microns) around the binder was clearly observed.

The major product formed under high alkalinity with <50 wt% of GGBFS was a geopolymeric gel similar to the one formed under low alkalinity. The microscopic analysis on such system has also indicated that there were small calcium precipitates (<10 microns) scattered around the sodium aluminosilicate phase as shown in Fig. 4. The absence of the formation of two separate phases in such a system indicated that the phase coexistence is dependent on the alkalinity used as well as the ratio between GGBFS and MK.

The current microscopic analysis confirmed the previous findings by Alonso and Palomo [10] that some forms of CSH gel were the main products when metakaolin was alkali activated in the presence of calcium hydroxide under low alkalinity. When the concentration of alkali hydroxide was increased from 5 M to 10 M, an amorphous alkaline aluminosilicate (geopolymer) would be formed as the dominant product with a small amount of CSH gel also being formed.

The current system is more complex with an amorphous calcium mineral (GGBFS) being used and soluble silicate source being added. Different glassy phases in GGBFS are expected to react at different rates. Moreover, the presence of minor elements, such as iron and sulphur could initiate other side reactions, resulting in the development of other minor products. Nevertheless, the results have reconfirmed that, provided the right condition is present, the formation of geopolymers and CSH gel can take place simultaneously.

### 3.3. Elemental analysis along the interfacial region between geopolymeric and CSH gels

In order to understand the chemical mechanism behind the coexistence of geopolymeric and CSH gels, a linescan analysis (marked as x–y in Fig. 1) detailing the changes in elemental composition was conducted across the two separate phases existing in Matrix M2. Fig. 5 shows the processed elemental concentration profile across the region. The standard deviations

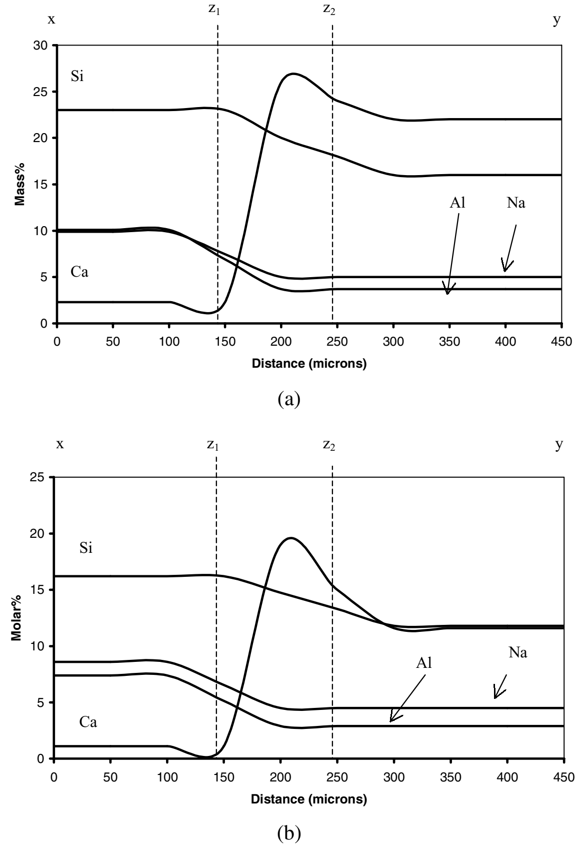

(a)

(b)

*Figure 5* An elemental line scan on x–y in Fig. 1 with (a) showing the mass composition and (b) showing the atomic composition.

TABLE IV EDS linescan analysis (atomic%, $x \pm \sigma_{n-1}$) for the interface between the aluminosilicate rich phase and the calcium rich phase (Line x–y) as shown in Fig. 1. The molar compositions of MK and GGBFS are also shown, based on Tables I and II

| Mole% | Oxygen (O) | Sodium (Na) | Aluminium (Al) | Silicon (Si) | Calcium (Ca) | *n* |
|---|---|---|---|---|---|---|
| Overall (x-y) | 66.5 ± 7.3% | 4.64 ± 33% | 3.99 ± 97% | 13.2 ± 40% | 9.98 ± 91% | 256 |
| Al-Si region (x-$z_1$) | 65.9 ± 5.5% | 8.55 ± 18% | 7.42 ± 26% | 16.2 ± 23% | 1.12 ± 71% | 101 |
| Interfacial region ($z_1$-$z_2$) | 66.1 ± 12% | 4.52 ± 31% | 3.84 ± 56% | 12.5 ± 47% | 17.0 ± 44% | 12 |
| Rich calcium region ($z_2$-y) | 67.5 ± 5.9% | 4.48 ± 36% | 2.86 ± 39% | 11.8 ± 37% | 11.6 ± 37% | 143 |
| MK | 63.2 | 0.05 | 16.3 | 18.8 | 0.04 | XRF |
| GGBFS | 58.3 | 0.22 | 6.41 | 13.3 | 17.8 | XRF |

$x$ = average atomic%, $\sigma$ = standard deviation in %, and $n$ = number of sample size.

in Table IV based on the elemental compositions in Fig. 5 showed that the concentration of each element was consistent within areas A and B, and that there was a narrow interfacial area ($z_1$–$z_2$) between the two regions. Apart from calcium and oxygen, the concentrations of all other elements, silicon, aluminium and sodium, were more concentrated in the aluminosilicate rich area (Area A, x-$z_1$) than in the calcium rich area (Area B, $z_2$-y).

Fig. 5 and Table IV show that the molar concentration of calcium increased 15 fold in less than 50 microns of space in the interfacial region. After a sharp increase in calcium concentration in the interfacial region, the concentration decreased to a lower but consistent level when it reached the bulk of area B. This has indicated that not only the materials in areas A and B were vastly different, but also that the calcium species in the interfacial region were substantially different from the CSH gel in the main body.

With the concentration of sodium in both raw materials being very low (<0.22 mol%), it is expected that the sodium found in both phases originated from the alkali activator (NaOH and sodium silicate). Sodium concentration in the geopolymeric gel was much higher than that in the calcium rich area. This has indicated that sodium added had a more prominent structurally determining role in the aluminosilicate gel than in the case of the CSH gel. This result is expected as sodium is required to play a charge-balancing role in the geopolymeric gel [2, 4–8, 17], while it is not generally required in forming the CSH gel.

The effect of alkali on ordinary Portland cement has been widely studied, partly due to the problems associated with the alkali-aggregate reaction and carbonation, which are believed to be some of the main causes of deterioration of modern concrete [3, 18]. However, no documented research has suggested that alkali will play a structurally determining role in forming CSH gel. Thus, the difference in the sodium concentration has also confirmed that the phases in areas A and B were vastly different. The presence of sodium in the CSH gel phase is likely to result from the formation of various sodium precipitates, e.g., sodium silicate, sodium carbonate, sodium sulphate and various forms of sodium aluminosilicate or aluminate.

The concentration of silicon did not vary much across the two phases, with the aluminosilicate gel having a higher silicon concentration than the calcium rich phase. The slightly higher concentration of oxygen in the calcium rich phase is suggested to be due to the presence of various forms of calcium silicate hydrate and calcium hydroxide in the region. The difference in aluminium concentration between the two regions was also significant.

The molar ratio between silicon and calcium in the calcium rich phase was about 1, while the molar ratio between the two species in the GGBFS was about 1.3 (Table IV). The molar ratios between aluminium and calcium in area B and in raw GGBFS were 0.25 and 0.36 respectively. The difference between these ratios in the calcium rich phase and raw GGBFS grain, as well as the presence of sodium in the region, indicated that the calcium rich phase was not just a large area of unreacted GGBFS grains. Some new calcium hydrated phases were the main products in region B.

The rapid increase in calcium concentration and decrease in aluminium concentration from the geopolymeric gel (A) to the calcium rich region (B), has indicated that during alkali activation, aluminium diffused out of region B and participated in forming the aluminosilicate in region A. The diffusion of aluminium from area B to A has been confirmed by the much lower Al:Ca ratio found in area B than in GGBFS grains. It is anticipated that dissolved calcium will bind with dissolved silicate preferentially in region B, which causes the dissolved aluminate species to diffuse out of area B and participate in the polymerisation with other silicate and aluminate dissociated from MK in forming geopolymeric gel in A.

The calcium content in region A has a high standard deviation, and appears to be unevenly distributed, perhaps owing to precipitated phase interspaced with the aluminosilicate. However, the standard derivations of the sodium, aluminium and silicon concentration are greater in region B than in A. This suggests that the calcium rich region consists of a greater variety of phases than the aluminosilicate region.

The atomic ratio between silicon and aluminium was slightly higher than 2, while the ratio between sodium and aluminium was slightly greater than 1 for the aluminosilicate region. According to the chemical designation of geopolymers as suggested by Davidovits [5], the resultant aluminosilicate phase formed in this binder (Matrix M2) would be similar to the poly(sialate-siloxo) $M_n$-(Si—O—Al—O—Si—O)$_n$ with Si:Al = 2:1 and Na:Al = 1:1. According to Davidovits [5], this type of geopolymer results from the chemical reaction at atmospheric pressure of geopolymeric precursors such as aluminosilicate oxides ($Al^{3+}$ in IV-fold coordination) with alkali polysilicate yielding polymeric Si—O—Al bonds. The conditions used in forming poly(sialate-siloxo) are similar to those used in synthesising the binders in this study. Apart from the presence of a low percentage of calcium within area A, this aluminosilicate gel formed appears to be similar to the standard poly(sialate-siloxo). Subsequently, despite the addition of moderate amounts of GGBFS, geopolymers were still the main products formed as a result of the alkali activation of MK. However, it is inconclusive to suggest the type of bonding between calcium and the aluminosilicate based on the SEM examination alone. It is unlikely that calcium will form a charge-balancing role in the same way as the sodium, as calcium will form calcium hydroxide and calcium silicate preferentially. The presence of calcium is suggested to be the result of the formation of calcium precipitates or the presence of undissolved GGBFS within the geopolymeric gel.

### 3.4. Microanalysis of hydration products

The elemental analyses of the different gel phases of the binders synthesised under Ms = 2.0 and 1.2 at 14 days are summarised in Tables V and VI. It should be noted that there was no clear phase separation occurring in some MK/GGBFS systems (namely Matrices M5, N2 and N3), so that the elemental analyses of the different gel phases for these matrices were estimated from areas with substantial difference in the concentration of calcium.

The average compositions of the aluminosilicate gel (Tables V and VI) were changing from $Na_{0.53}Ca_{0.07}SiAl_{0.46}$ (20% GGBFS) to $Na_{1.1}Ca_{0.5}SiAl_{0.24}$ (80% GGBFS) for Ms = 2.0, and from $Na_{0.89}Ca_{0.05}SiAl_{0.46}$ (20% GGBFS) to $Na_{1.7}Ca_{0.25}SiAl_{0.24}$ (80% GGBFS) for Ms = 1.2.

It can be observed that the $Al_2O_3/SiO_2$ (A/S) ratio of the aluminosilicate rich gel decreased as the GGBFS content increased. This trend is expected as most aluminium was originating from MK, so that as the MK/(MK + GGBFS) ratio decreased, the amount of aluminium present in the system also decreased accordingly.

In addition, the Na:Si and Ca:Si ratios increased as the aluminium content decreased in the aluminosilicate rich phase. This may be due to excess silicate in the aluminosilicate rich phase resulting from the lack of aluminium available for polymerisation. The lack of dissolved aluminium species in the solution phase has hindered any further formation of large silicate oligomers. The demand for calcium and sodium within the structure increases in order to balance the negative charge within the shorter silicates chain.

As the amount of sodium hydroxide increased in the system, less calcium would be available to react with

TABLE V SEM EDS analysis (atomic ratios, $x \pm \sigma_{n-1}$) for rich aluminosilicate phase and rich calcium phase in 14 days old MK-GGBFS binders synthesised using Ms = 2.0

| | Matrix | $CaO/SiO_2$ | $Al_2O_3/Na_2O$ | $Al_2O_3/SiO_2$ | *n* |
|---|---|---|---|---|---|
| Rich calcium phase | M1 | – | – | – | – |
| | M2 | 0.99 ± 2.8% | 0.88 ± 10% | 0.12 ± 17% | 75 |
| | M3 | 0.96 ± 3.7% | 0.79 ± 12% | 0.12 ± 24% | 50 |
| | M4 | 0.91 ± 5.3% | 0.42 ± 18% | 0.10 ± 7.8% | 60 |
| | M5 | 1.12 ± 11% | 0.21 ± 78% | 0.14 ± 39% | 64 |
| | M6 | 1.20 ± 20% | 0.19 ± 110% | 0.10 ± 41% | 70 |
| Rich aluminosilicate phase | M1 | 0 | 0.85 ± 7.0% | 0.26 ± 6.6% | 75 |
| | M2 | 0.07 ± 26% | 0.87 ± 14% | 0.23 ± 15% | 63 |
| | M3 | 0.08 ± 36% | 0.97 ± 54% | 0.21 ± 28% | 40 |
| | M4 | 0.15 ± 21% | 0.54 ± 16% | 0.16 ± 7.0% | 50 |
| | M5 | 0.48 ± 46% | 0.21 ± 140% | 0.12 ± 27% | 68 |
| | M6 | – | – | – | – |

x = average atomic%, $\sigma$ = standard deviation in %, and *n* = number of sample size.

TABLE VI SEM EDS analysis (atomic ratios, $x \pm \sigma_{n-1}$) for rich aluminosilicate phase and rich calcium phase in 14 days old MK-GGBFS binders synthesised using Ms = 1.2

| | Matrix | $CaO/SiO_2$ | $Al_2O_3/Na_2O$ | $Al_2O_3/SiO_2$ | *n* |
|---|---|---|---|---|---|
| Rich calcium phase | N1 | – | – | – | – |
| | N2 | 1.00 ± 25% | 2.40 ± 21% | 0.23 ± 7.8% | 15 |
| | N3 | 0.97 ± 16% | 1.65 ± 7.8% | 0.21 ± 8.6% | 15 |
| | N4 | 1.01 ± 1.8% | 0.25 ± 40% | 0.10 ± 26% | 50 |
| | N5 | 1.11 ± 4.9% | 0.22 ± 40% | 0.10 ± 7.2% | 50 |
| | N6 | 1.19 ± 1.6% | 0.20 ± 38% | 0.10 ± 15% | 50 |
| Rich aluminosilicate phase | N1 | 0 | 0.73 ± 12% | 0.35 ± 2.3% | 45 |
| | N2 | 0.05 ± 39% | 0.51 ± 19% | 0.23 ± 15% | 60 |
| | N3 | 0.04 ± 70% | 0.29 ± 32% | 0.15 ± 26% | 55 |
| | N4 | 0.23 ± 22% | 0.32 ± 3.7% | 0.15 ± 39% | 48 |
| | N5 | 0.25 ± 63% | 0.15 ± 14% | 0.12 ± 30% | 45 |
| | N6 | – | – | – | – |

x = average atomic%, $\sigma$ = standard deviation in %, and *n* = number of sample size.

the silicate and aluminate. Instead, calcium would precipitate out as calcium hydroxide, then participate in the formation of CSH gel. It has been confirmed by the microscopic and elemental analysis along the interfacial region between the two phases that various calcium precipitates were formed.

The $CaO/SiO_2$ (C/S) molar ratios of CSH gel in most kinds of cementitious systems have been well studied using different techniques such as phase equilibrium, extraction techniques and analytical electron microscopy. There are a large number of crystalline, semi-crystalline and amorphous CSH phases possible as a result of the hydration of cement [3]. Taylor [3] argued that the complexity of the $CaO\text{-}SiO_2\text{-}H_2O$ system lies in the greater ionic radius and more electropositive character of calcium, which permits different types of coordination with oxygen.

Tables V and VI show that the molar ratios between calcium, silicon, aluminium and sodium varied according to the ratios between the MK and GGBFS added initially. For matrices M1 to M6 synthesised at $Ms = 2.0$, the C/S ratios of the calcium rich phase were relatively consistent, varying from $\sim 0.9$ to $\sim 1.2$. As a general trend, the C/S ratio increased with increasing GGBFS content in the binder. The same trend was observed in the C/S ratios in the aluminosilicate rich phase and also in the corresponding ratios for matrices synthesised using $Ms = 1.2$.

Richardson [19] found that the C/S ratio of CSH in neat Portland cement pastes varies from $\sim 1.2$ to $\sim 2.3$ with a mean of $\sim 1.75$. These numbers are higher than those found in this investigation. It is concluded that the nature of calcium silicate hydrates formed in the binders studied was different from the normal CSH gel formed in Portland cement and also the amorphous calcium silicate present in the raw slag. However, as the alkalinity of the alkali activator decreased, the characteristics of CSH gel formed increasingly resembled the CSH in Portland cement.

Table VI shows that for the calcium rich phase synthesised at high alkalinity ($Ms = 1.2$) and with moderate amounts of GGBFS (Matrices N2 and N3), the $Al_2O_3/Na_2O$ ratios were substantially higher than in other matrices or in the aluminosilicate region. It is suggested that the high aluminium content resulted from a high concentration of unreacted GGBFS grains present in the region. Subsequently, it is anticipated that the presence of large amounts of sodium hydroxide could inhibit the possible formation of calcium silicate hydrate. A detailed discussion on the effect of excess sodium hydroxide in inhibiting the growth of CSH gel will be presented below.

### 3.5. Proposed mechanism of alkaline activation of MK in the presence of GGBFS

It was found from this study that the alkali activation of MK in the presence of GGBFS is highly dependent on the alkalinity of the alkali activator and the ratio between MK and GGBFS. The microscopic analysis has shown that given the right condition, two separate phases—a calcium silicate phase and a sodium aluminosilicate will be formed simultaneously in the alkali activation process.

It is often argued that dissolution of aluminosilicate minerals is the first step of geopolymerisation [2, 17]. In the current study, it is anticipated that when both MK and GGBFS are mixed with the alkali activator (sodium hydroxide and sodium silicate solution), dissolution is also the first reaction to take place. Silicon and aluminium will be dissolved from the surface of MK and at the same time silicon, aluminium and calcium will be dissolved from the surface of GGBFS. The rate of dissolution from each mineral is dependent on the concentration of sodium hydroxide used. Therefore, it is anticipated that the dissolution rate of MK and GGBFS at different alkalinity will determine the ratios of the dissolved species present in the system. The nature and amount of dissolved species present in the suspension will determine the subsequent reaction or reactions to take place, which are expected to include polymerisation and various other precipitation processes.

When alkaline solution activates the surface of the GGBFS, calcium and silicon dissolve from the GGBFS surface. It was found from the current study that dissolved calcium from GGBFS would take part in the formation of CSH gel in preference to participating in the polymerisation with aluminosilicate. It can be concluded that dissolved calcium from GGBFS plays a similar role to the calcium hydroxide as suggested by Alonso and Palomo [9, 10] in the alkaline activation of MK, that leads to the formations of amorphous and semi-crystalline sodium aluminosilicate with some forms of CSH gel as a secondary product.

In the presence of aqueous sodium hydroxide, the surface of GGBFS particles will be saturated with the hydroxyl ion. It is anticipated that when calcium dissolves from GGBFS, it will diffuse out of the GGBFS grain and will further react with hydroxyl ion and precipitate as $Ca(OH)_2$. When there is a substantial amount of calcium hydroxide present around the surface of GGBFS, it will make the diffusion of dissolved calcium out of the GGBFS even more difficult. Since the diffusion of calcium from GGBFS to aluminosilicate is restricted, excess dissolved calcium will remain intact within the GGBFS grain and form a new nucleation centre, in which amorphous calcium silicate hydrate will be produced and grown within the region. The lack of dissolved calcium present in the aluminosilicate body will inhibit any formation of calcium aluminosilicate hydrate. It is suggested that the presence of the small amount of dissolved calcium will react with soluble silicate and precipitate on the surface of a geopolymeric gel. As a result, two distinct phases will be produced in such a system and substantial amounts of calcium hydroxide or various other types of calcium precipitate will be formed along the interfacial area as shown in the current investigation.

Under low NaOH concentration, layers of hydroxyl ions and calcium hydroxide will not be too thick along the interfacial area, so that a small amount of dissolved calcium will be able to diffuse out of the layers if there is a relatively high amount of dissolved calcium present in the system. Tables V and VI show that in general the $CaO/SiO_2$ ratios of the rich aluminosilicate phase were higher in matrices synthesised under Ms = 2.0.

Phair and van Deventer [20] showed that the solubility of calcium decreased with increasing pH owing to the formation of calcium hydroxide. With a decreased amount of calcium hydroxide formed in the system, more calcium will be available to react with soluble silicate in forming calcium silicate hydrate. Moreover, previous findings from Xu and van Deventer [17] showed that the dissolution of silicon and aluminium from various aluminosilicate minerals is slower in alkali activator of lower $OH^-$ concentration. Hence the formation of calcium silicate hydrate is favoured as the initial amount of dissolved aluminate is not enough to promote the formation of calcium aluminosilicate. In addition, since the layers of hydroxyl ions and calcium hydroxides around the surface of the rich calcium silicate region are weak, more space is available for the nucleation and growth of CSH in the region. Thus, the growth of CSH will be promoted and a clear region of calcium rich area could be distinguished microscopically.

In contrast, when more sodium hydroxide is added to the system, dissolved calcium species will not participate in the formation of calcium silicate hydration, or only a limited amount of dissolved calcium will participate in the formation of CSH, which makes its presence difficult to be observed microscopically. Instead, calcium hydroxide will be precipitated out, and this will inhibit any possibility for dissolved calcium to participate in the formation of CSH. With decreasing amounts of dissolved calcium present, the formation of CSH gel is not possible unless a higher amount of calcium source is added to the system initially. Thus, when more GGBFS was added in the current study (more than 60%), a clear coexistence of the two phases could be observed. Moreover, as the layers of calcium hydroxide and hydroxyl ions are much thicker in systems where high alkalinity was used, the lack of physical space around the GGBFS grain has also restricted any possible growth of CSH. Subsequently, scattering of small calcium precipitates ($<10$ microns) around the sodium aluminosilicate phase was observed instead in this study. This also explains why more unreacted GGBFS was present in the matrices N2 and N3.

### 3.6. Effect of coexistence of geopolymeric gel and calcium silicate hydrate on durability of resultant binder

The results found in the current study have shown that given the right condition, it is possible to have both amorphous alkali aluminosilicate and CSH gel forming simultaneously within the same system. As suggested by Glukhovsky [1], the long-term stability of concrete results from the presence of analcime (alkaline silico-aluminohydrates) and CSH gel rather than CSH gel alone. It is suggested that analcime (alkaline silico-aluminohydrates) is similar to the alkali aluminosilicate (geopolymer) produced as a result of the alkali activation of MK. If the hypothesis of Glukhovsky is correct, then the binder formed here with the coexistence of both geopolymeric and CSH phases, will be the modern version of ancient concrete.

The alkaline activation of MK in the presence of a calcium source causes the two reactions to take place simultaneously. It is anticipated that the amount, nature and size of the two phases present will determine the initial mechanical properties of the resultant matrices. The amount, nature and size of the hydration products can be controlled by using different types of aluminosilicate and calcium source, different ratios between aluminosilicate and calcium source, and a different type and quantity of alkali activator.

It was found from a previous study [15] that the addition of excessive amount of GGBFS has a negative effect on the mechanical properties of the resultant binders. Thus, even though it is possible to form CSH and geopolymeric gels simultaneously in a highly alkaline system (Ms = 1.2) by adding substantial amounts of GGBFS as shown in this study, the mechanical properties of the resultant binder will not be improved merely having these two phases present. It is suggested that the presence of unstable phases such as calcium hydroxide and various other calcium precipitates along the interfacial area may also affect the long-term stability and interaction between the CSH and geopolymeric gels. It is hypothesised that the presence of these precipitates will further promote reactions between the geopolymeric gel and CSH gel, in which it will determine and enhance the durability of such binder.

## 4. Conclusion

It is proposed that the coexistence of geopolymeric and CSH gels and the reactivity of the interfacial zone between the two phases will hold the key in reinventing a construction material that will match the durability of ancient concrete. A chemical mechanism has been proposed on how the presence of GGBFS in the alkali activation of MK could result in the formation of two separate phases, namely geopolymers and CSH gel.

CSH gel formed in such system had a significantly lower Ca/Si ratio than the CSH commonly formed from the hydration of ordinary Portland cement. There were some calcium precipitates along the interfacial region between the CSH and geopolymeric gel. It is suggested that the properties (e.g., size, elemental composition) of geopolymeric gel and CSH gel formed simultaneously, and the reactivity of the calcium precipitates along the interfacial region, will determine the durability of such binder.

## Acknowledgements

The financial support received from the Australian Research Council (ARC), the Particulate Fluids Processing Centre, a Special Research Centre of the ARC, and the US Air Force Office of Scientific Research/ Asian Office of Aerospace Research and Development (AOARD), under Contract AOARD 02-33, is greatly appreciated.

## References

1. V. D. GLUKHOVSKY, in Proceedings of the Alkaline Cements and Concrete, Kiev, Ukraine, 11–14 October 1994, edited by P. V. Krivenko (VIPOL Stock Company, 1994) p. 1.
2. P. V. KRIVENKO, in Proceedings of the Alkaline Cements and Concrete, Kiev, Ukraine, 11–14 October 1994, edited by P. V. Krivenko (VIPOL Stock Company, 1994) p. 11.
3. H. F. W. TAYLOR, "The Chemistry of Cements" (Academic Press, 1964).
4. J. DAVIDOVITS, *J. Thermal Anal.* **37** (1991) 1633.
5. *Idem.*, in CD Proceedings of the Second International Conference on Geopolymers, Universite de Picardie, Saint Quentin, France, 30 June–2 July, 1999.
6. J. DAVIDOVITS, D. C. COMRIE, J. H. PATERSON and D. J. RITCEY, *Concrete Int.* July (1990) 30.
7. J. G. S. VAN JAARSVELD, PhD thesis, The University of Melbourne, 2000.
8. J. DAVIDOVITS and M. DAVIDOVICS, *Ceram. Eng. Sci. Proc.* **9**(7/8) (1988) 835.
9. S. ALONSO and A. PALOMO, *Mater. Lett.* **47** (2001) 55.
10. *Idem.*, *Cem. Concr. Res.* **31** (2001) 25.
11. M. FRIAS, M. I. SANCHEZ DE ROJAS and J. CABRERA, *ibid.* **30** (2000) 209.
12. J. CABRERA and M. F. ROJAS, *ibid.* **31** (2001) 177.
13. N. J. COLEMAN and W. R. MCWHINNIE, *J. Mater. Sci.* **35** (2000) 2701.
14. M. FRIAS and J. CABRERA, *Cem. Concr. Res.* **31** (2001) 519.
15. C. K. YIP and J. S. J. VAN DEVENTER, in CD Proceedings of the 6th World Congress of Chemical Engineering, Melbourne, 24–27 September 2001.
16. A. C. NEWMAN, "Chemistry of Clays and Clay Minerals" (Longman Scientific & Technical, 1987).
17. H. XU and J. S. J. VAN DEVENTER, *Int. J. Miner. Process.* **59** (2000) 247.
18. M. S. J. GANI, "Cement and Concrete" (Chapman & Hall, 1997).
19. I. G. RICHARDSON, *Cem. Concr. Res.* **29** (1999) 1131.
20. J. W. PHAIR, J. S. J. VAN DEVENTER and J. D. SMITH, *Ind. Eng. Chem. Res.* **39** (2000) 2925.

*Received 15 July 2002*
*and accepted 10 June 2003*